Postprint of: Mikielewicz J., Mikielewicz D., A simplified energy dissipation based model of heat transfer for post-dryout flow boiling, International Journal of Heat and Mass Transfer, Vol. 124 (2018), pp. 260-268, DOI: 10.1016/j.ijheatmasstransfer.2018.03.063

Manuscript submitted for consideration to publish in International Journal of Heat and Mass Transfer

A simplified energy dissipation based model of heat transfer for post – dryout flow boiling

Jarosław Mikielewicz[a], Dariusz Mikielewicz[b]

[a] Institute of Fluid-Flow Machinery, Polish Academy of Science, 80-231 Gdańsk, ul. Fiszera 14, Poland

[b] Gdansk University of Technology, Faculty of Mechanical Engineering, 80-233 Gdańsk, ul. Narutowicza 11/12, Poland

Abstract

A model for post dryout mist flow heat transfer is presented based on considerations of energy dissipation in the flow. The model is an extension of authors own model developed earlier for saturated and subcooled flow boiling. In the former version of the model the heat transfer coefficient for the liquid single-phase convection as a reference was used, due to the lack of the appropriate model for heat transfer coefficient for the mist flow boiling. That issue was a fundamental weakness of the former approach. The purpose of present investigation is to fulfil this drawback. Now the reference heat transfer coefficient for the saturated flow boiling is that corresponding to vapour flow the end of the mist flow. The wall heat flux is based on partitioning and constitutes of two principal components, namely the convective heat flux for vapour flowing close to the wall and two phase flow droplet–vapour in the core flowing. Both terms are accordingly modelled. The results of calculations have been compared with some experimental correlations from literature showing a good consistency.

Keywords: post dryout, mist flow, modeling

NOMENCLATURE

Bo - Boiling number, $B=q/(G\, h_{lv})$

c - specific heat [J/(kgK)]

C - constant

D_h - hydraulic diameter [m]

E - energy dissipation [W/m^3]

f - friction factor

g - gravitational acceleration [m^2/s]

G - mass velocity, [$kg/(m^2s)$]

h_{lv} - latent heat [J/kg]

$\dot{m}$ - mass flow rate, kg/s

p - pressure [N/m^2]

P - empirical correction, perimeter

R - tube radius [m]

q - heat flux [W/m^2]

r -radius [m]

Re - Reynolds number, $Re=G\ D_h/\mu_l$

T - temperature [^oC]

x - quality [-]

z - wall normal coordinate [m]

Greek symbols

α - heat transfer coefficient [$W/(m^2K)$]

λ - thermal conductivity [(W/mK)]

μ - dynamic viscosity [kgm/s]

ρ - density [kg/m^3]

σ - surface tension [kg/s^2]

τ - shear stress [N/m^2]

subscripts

A - annular

AV - annular vapour

c - core

e - equivalent

l - liquid phase

K - two-phase core

M - mist

O - reference

p - constant pressure

Pb - pool boiling

ref - reference

sat - saturation
TP - two-phase
TPB - two-phase flow boiling
v - vapour
w - wall

superscripts
+ - non-dimensional

1. Introduction

The flow boiling for a long time has been perceived as one of the most effective ways of removal of large heat fluxes. The phenomenon found applications in various areas of technology where efficient cooling is required. Examples of such applications are nuclear reactor cooling, medical applications where cooling of neutron generators used in treatment of tumours is necessary, testing of materials, cooling of electronic equipment or cooling of gas turbine nozzles.

In the annular-mist flow with heated walls, the liquid film is depleted by both the entrainment of liquid droplets and by the evaporation. When the liquid film experiences almost complete depletion and no longer covers the wall, the heat transfer between the fluid and the channel wall deteriorates, leading to the onset of boiling crisis called dryout. As the flow develops further downstream in the post-dry out region, the liquid flows only as droplets in the core flow, and the channel wall temperature increases to a higher level. This phenomenon has made the prediction of the heat transfer in mist (dispersed) flow regime more complicated and more difficult. In the case of the post-dry out heat transfer, where droplets are travelling in the core of the flow forming the mist with vapour, due to the fact

that heat is not transferred directly from the heated wall to the liquid droplets; instead, the heat is first transferred to the vapour next to the wall. Subsequently only a part of that heat is transferred from the vapour to the liquid droplets, which leads to different temperatures between liquid droplets and the vapour phase. In such case, significant amounts of liquid droplets may exist even though the equilibrium quality exceeds unity. As a result of that temperature of non-equilibrium vapour becomes superheated, where superheat of vapour phase may reach few hundreds Kelvins. The dryout occurrence and the downstream post-dry out wall temperature excursion could damage the channel wall. Because of this reason, exact mechanisms for the heat transfer process are still poorly understood and reliable prediction models are still being sought. Such situation is present even though numerous experimental measurements and prediction models have concentrated on the dispersed flow heat transfer.

A number of papers in the literature are devoted to this issue but the complexity of the process makes the analysis of that case very challenging. Several modelling approaches have been developed to predict the heat transfer rate during mist flow boiling. Such models can be generally divided into two categories, namely purely empirical correlations for heat flux calculations or the formulas based on mechanistic models. The empirical approaches express the wall heat flux or partitioning of the wall heat flux. Non-consistent empirical correlations for heat transfer coefficient are used for expressing a particular wall heat flux partitioning. Non-consistency partially stem from the fact that empirical correlations are generally limited to particular flow conditions. Hence empirical correlations do not include modelling of the heat transfer mechanisms. The alternative are the mechanistic models which are capable of determining the particular heat flux components individually. Usually main aspects of the problem are studied. Firstly the distance from the dryout conditions to the complete evaporation of the drops in the core flow and, secondly, heat transfer from the wall to fluid. Hence empirical correlations for wall heat flux partitioning can only provide information

regarding how the wall heat flux is to be partitioned. They cannot be used for the prediction of the wall heat flux itself. The mechanistic models, on the other hand, which are based on the relevant heat transfer mechanisms occurring during the boiling process, have the capability for individual determination of each of the relevant heat flux components. Hence the mechanistic models can be used for both the prediction of the wall heat flux and the partitioning of the wall heat flux between the liquid and vapour phases. An excellent review of literature on the topic of empirical correlations for heat flux, empirical correlation for partitioning of wall heat flux and mechanistic models for prediction of wall heat flux and partitioning can be found in [1].

The region of the mist zone can be either large or small in relation to the fluid properties, mass flux, pressure and heat flux. It is a non-equilibrium region in which the quality and void fraction are positive non-zero values but the vapour temperature is above the saturation temperature. Modelling of such phenomenon represents significant difficulties.

Nishikawa et al [2] investigated critical heat flux and heat transfer coefficient in relation to the safety and performance of vapour generators at high subcritical pressure with refrigerant R22 as working fluids. They introduced the Knudsen number Kn to take account of the thermodynamic non-equilibrium between the vapour and the liquid droplets, correcting in such way the wall temperature distributions. The proposed model predicted satisfactorily heat transfer to R22 at high subcritical pressures.

Jones Jr and Zuber [3] shown that the non-equilibrium component of the total energy can be expressed as a first-order, inhomogeneous relaxation equation in terms of the newly introduced parameter named the superheat relaxation number. That model proved to show that the effects of mass velocity and heat flux along the length of the tube for equilibrium qualities from 0.13 to over 3.0.

Terekhov et al [4] studied the steam-drop flow in a tube. Authors postulated the factors influencing the heat and mass transfer process in steam-drop flow. These were initial mass concentration of liquid droplets, their initial diameter, mixture velocity, heat flux, initial temperature of steam flow. They found that the evaporation rate of particles increases with increasing heat flux and initial vapour temperature, whereas the decreasing trend is observed with increasing droplet size. Considerations enabled to estimate the distance over which all droplets evaporated.

Guo and Mishima [1] claim that it is impossible to predict accurately the heat transfer in the mist flow without considering the thermal non-equilibrium between droplets and vapour. Authors considered five configurations of interaction between vapour, liquid droplets and the wall. These were forced convection of vapour phase to the wall, the direct contact heat transfer of droplets to the wall, the interfacial heat transfer between vapor and droplets and the radiation between the wall, droplets and vapour. It resulted from this study that the heat transfers by radiation and by direct droplet contact to the wall are important under low pressure and low mass flow conditions. Neglecting these two heat transfer paths may lead to an unacceptable error in wall temperature prediction. Nevertheless the vapour convection is the dominant heat transfer mechanism.

Liu and Anglart [5] suggested an integrated CFD model to include both the pre-dryout annular-mist flow and the post-dryout mist flow, with post-dryout heat transfer accounted for. The three-field annular-mist CFD model couples the thin liquid film model with the two-field two-fluid model of the gas core flow including the gas phase and the droplets. The dryout occurrence was predicted using a critical film thickness model. The various post-dryout heat transfer mechanisms were identified and calculated to give the wall and the fluid temperatures.

Caha and Krejci [6] developed a thermal-hydraulic procedure based on isolated channel model was developed. It includes a wide range of heat transfer correlations for different one phase and two phase flow regimes.

The objective of the present work is to devise a model for calculation of the convective part of heat transfer coefficient in mist flow boiling developed on the basis of energy dissipation principle in the flow under thermal equilibrium conditions. In such conditions heated surface is cooled by forced convection of vapour only and the radiation effects are omitted. The resultant model of mist flow model is a modification to the saturation flow boiling developed earlier by the authors, presented in detail in [7–10]. In addition the heat flux due to evaporation of droplets in core flow has been determined. The droplets are evaporating until disappear in the end in longitudinal direction Fig. 1.

2. Semi-empirical modelling of flow boiling

Presented analysis will be derived from the original concept of flow boiling modelling applied to saturated flow conditions. J. Mikielewicz (1973) [7]. In that approach the heat transfer coefficient in the saturated flow boiling was devised in terms of the simpler modes of heat transfer namely the single phase heat transfer and pool boiling heat transfer as well as a two-phase flow multiplier, which is a distinct feature of the model. The end of the process of flow boiling modelling was referenced to the forced convection value in the vapour phase flow. Such approach is not physically correct. As the boiling process reaches dryout conditions the mist flow is created and the equilibrium quality equal one is assumed regardless of the fact that the core contains still droplets. Therefore the model presented in the following attempts to determine the heat transfer coefficient for equilibrium quality equal one

and the distance to the end of the mist flow. In author's previous papers [7-10], concerning saturated flow boiling; we used the heat transfer coefficient for the vapour single-phase flow as the heat transfer coefficient in the end of the flow boiling process. Therefore that issue was a fundamental weakness of the model developed in earlier approaches. The purpose of present investigation is to improve this drawback.

2.1. Fundamentals of semi-empirical method of determination of heat transfer coefficient for post critical heat transfer.

In the case of mist flow boiling the same fundamental hypothesis can be applied as in the case of saturated flow boiling [7]. The saturated flow boiling model states that the total energy dissipation in the saturated flow boiling with bubble generation, treated as an equivalent flow of fluid with properties of the two phase flow, can be modelled as a sum of two contributions, namely the energy dissipation due to convective flow without bubbles, E_{TP}, and dissipation resulting from bubble generation, E_{Pb}. Similar terms can be considered in case of the mist flow boiling that means convective term of vapour flowing close to the wall, $E_{TP,K}$, and term due to two- phase dissipation in the mist flow in the core, E_{AV}. Hence the analysis of energy dissipation of mist flow constitutes the following hypothesis:

$$E_{TPB,M} = E_{TP,K} + E_{AV} \tag{1}$$

Energy dissipation under steady state conditions in the mist flow can be approximated by the energy dissipation in the laminar boundary layer for annular vapour flow, which dominates the heat and momentum transfer in the considered process. Analogically can be expressed the energy dissipation due to the two-phase flow in core flow. These energies are defined as the

power lost in the control volume, which can further be expressed as the ratio of square of shear stress to the dynamic viscosity in the boundary layer.

$$E = \frac{\tau^2}{\mu} \tag{2}$$

Substituting the respective expressions for energies into (1) a geometrical summation between respective shear stresses in mist flow corresponding wall shear stresses is obtained:

$$\tau_{TPB,M}^2 = \tau_{TP,K}^2 + \tau_V^2 \tag{3}$$

Utilizing the analogy for separate processes, namely the convection in annular vapour flow and mist flow in core treated as homogenous two- phase flow between the momentum and heat transfer we can generalize the above result to extend it over to heat transfer coefficients to yield the heat transfer coefficient in mist regime flow boiling in terms of simpler modes.

$$\alpha_{TPB,M}^2 = \alpha_{TP,K}^2 + \alpha_V^2 \tag{4}$$

Eq. (4) presents a geometrical summation of convective heat transfer coefficient in annular vapour flow and evaporating mist flow one in core.

2.2. Modelling of mist flow boiling.

The post dryout schematic of the flow is presented in Fig. 1. In the analysis we assume that:

1. Droplets and vapour in the core are flowing with the same velocities.
2. Quality and void fraction of the core flow are not changing, however due to evaporation of droplets the volume of the core is reducing its size.
3. Quality and void fraction in the core are the same as at the dryout location.

4. Core flow can be modelled as the homogenous two phase flow.
5. Distribution of shear stresses in vapour annular flow and two phase flow in core are linear.
6. Analogically linear distribution is applied for wall heat flux.

For homogenous flow in core the relationship is obeyed:

$$\frac{\varphi_c}{1-\varphi_c}\frac{\rho_v}{\rho_l} = \frac{x_c}{1-x_c} \tag{5}$$

Mass balance in the mist flow consists of the mass flow rate of the core, $\dot{m}_{TP,K}$, and the mass flow rate of vapour between the core and the wall, $\dot{m}_{TP,A}$, and gives:

$$\dot{m}_{TP,M} = \dot{m}_{TP,K} + \dot{m}_{TP,A} \tag{6}$$

The mass flow rate of the core consists of the mass flow rate of droplets in the core, $\dot{m}_{K,l}$, and vapour, $\dot{m}_{K,v}$:

$$\dot{m}_{TP,K} = \dot{m}_{K,l} + \dot{m}_{K,v} \tag{7}$$

Rate of heat supplied to the droplets in the core goes on to their evaporation (at the same time the radius of the core reduces its size). The energy balance on the element of the flow of droplets in the core, where heat flux is supplied from the wall, and transport of heat in the vapour around core is varying linearly, yields:

$$d\dot{m}_{K,l} h_{lv} = 2\pi r_i q_i dz \text{ where } q_i = q_w \frac{r_i}{R} \tag{8}$$

The elementary change in the mass of droplets can be expressed with respect to the total mass of the core using the definition of core quality, $x_c = \dot{m}_{K,v} / \left(\dot{m}_{K,v} + \dot{m}_{K,l}\right)$:

$$d\dot{m}_{K,l} = (1-x_c)d\dot{m}_{TP,K} = \frac{2\pi r_i q_w}{h_{lv}}\frac{r_i}{R}dz \tag{9}$$

The mass flow rate of droplets in the core can be expressed using the continuity equation as:

$$\dot{m}_{TP,K} = \pi r_i^2 w_{TP}\rho_{TP} \tag{10}$$

And hence the elementary change of the mass flow rate of droplets in the core reads:

$$d\dot{m}_{TP,K} = 2\pi\rho_{TP} w_{TP} r_i dr_i + \pi r_i^2 \rho_{TP} dw_{TP} \tag{11}$$

Introducing (11) into (9) enables to obtain the relation for the change of core radius with the distance from the dryout location:

$$\frac{dr_i}{dz} = \frac{2r_i q_w}{(1-x_c)w_0\rho_{TP}\left[-2w_{TP}(r_i) + r_i\frac{dw_{TP}(r_i)}{dr_i}\right]h_{lv}} \tag{12}$$

Equation (12) requires for its solution information about the velocity distribution. That requires consideration of mass balance of the vapour exchanging between the core and the vapour flowing close to the wall. Let's assume therefore that vapour is drifting the drops with mean velocity $w_{TP}(r_i)$ and due to their evaporation on the infinitesimal distance dz vapour is generated from the core flow (10):

$$d\dot{m}_{K,v} = \left(2\pi r_i w_{TP}\rho_{TP} dr_i + \pi r_i^2 \rho_{TP} dw_{TP}\right)x_c \tag{13}$$

In order to obtain the two-phase flow velocity the balance of mass flow in annular region for vapour flow can be formulated:

$$\dot{m}_{A,v} = \pi(R^2 - r_i^2)\rho_v w_{TP} \tag{14}$$

Differentiating equation (14) with respect to r and w_{TP} we get (assuming $dm_{K,v}=dm_{A,v}$):

$$d\dot{m}_{A,v} = -2\pi w_{TP}\rho_v r_i dr_i + \pi(R^2 - r_i^2)\rho_v dw_{TP} \tag{15}$$

Rearranging and combining (13) and (15) we arrive at:

$$\frac{dw_{TP}}{dr_i} = -\frac{2\left(\frac{\rho_{TP}}{\rho_v} - 1\right) r_i w_{TP}}{(R^2 - r_i^2) + r_i^2\left(\frac{\rho_{TP}}{\rho_v} - 1\right)} \tag{16}$$

Separating variables in (16) we obtain solution assuming that for: $r_i=0 \rightarrow w_{TP}=w_0$. Such condition is assumed at the end of the process of droplet evaporation, i.e. the core of the flow contains no droplets, and w_0 is the velocity of vapour without droplets:

$$w_{TP} = w_0\left[1 + a\left(\frac{r_i}{R}\right)^2\right]^{-1} = w_0\left[1 + a\left(r_i^+\right)^2\right]^{-1} \tag{17}$$

where: $w_0 = \frac{\dot{m}}{\pi R^2 \rho_v}$, $a = \frac{\rho_{TP}}{\rho_v} - 1$, $\frac{1}{\rho_{TP}} = \frac{x_c}{\rho_v} + \frac{(1-x_c)}{\rho_l}$, $r^+ = \frac{r}{R}$.

Introducing (17) into (12) we can find variation of the interface radius with respect distance z counting from the location of dry out:

$$\frac{dr^+}{dz^+} = \frac{2A}{-2\frac{w_{TP}^+}{r^+} + \frac{dw_{TP}^+}{dr^+}} \tag{18}$$

Substitution of the velocity distribution (17) and its derivative into (18) leads to the differential equation of the form:

$$-\frac{\left[1 + 2a\left(r^+\right)^2\right]}{r^+\left[1 + a\left(r^+\right)^2\right]^2} dr^+ = A dz^+ \tag{19}$$

Equation (19) has an analytical solution with respect to core radius r (z):

$$z^+ = \frac{-\ln\left(r^+\right)}{A} + \frac{\ln\left(\frac{1 + a\left(r^+\right)^2}{a}\right)}{2A} - \frac{1 + a\left(r^+\right)^2}{2A} + C \tag{20}$$

where: $r^+ = \frac{r}{R}$, $z^+ = \frac{z}{R}$, $A = \frac{q_w}{(1-x_c)\rho_{TP} w_0 h_{lv}}$, $w_{TP}^+ = \frac{w_{TP}}{w_0}$.

The constant C can be evaluated from the initial condition, that for $z^+=0$ the radius of the core is equal to $r^+=1$. Hence the constant C is:

$$C = -\frac{\ln(1/a)+1}{2A} \tag{21}$$

Relation (20) combined with (21) allows calculating radius of interface between two phase core and annular vapour region with respect to distance z and in final form reads:

$$z^+ = \frac{\ln\left[\frac{\left[\frac{1+a\left(r^+\right)^2}{r^+}\right]^{1+a\left(r^+\right)^2}}{\exp\left[a\left(r^+\right)^2\right]}\right]}{2A\left[1+a\left(r^+\right)^2\right]} \tag{22}$$

The equilibrium quality x_e can be derived from the definition:

$$x_e = \frac{\dot{m}_{vv}}{\dot{m}} = \frac{\pi(R^2 - r_i^2)\rho_v w_{TP} + \pi r_i^2 \rho_{TP} w_{TP} x_c}{\dot{m}_{vv} + \dot{m}_{TP,K}} \tag{23}$$

Hence the relation between the core flow radiuses against quality x_e reads:

$$r^+ = \frac{r_i}{R} = \sqrt{\frac{1+\left(\frac{x_c}{1-x_e}\right)}{1+\left(\frac{1+x_c}{1-x_e}\right)\frac{\rho_{TP}}{\rho_v}}} \tag{24}$$

Relation (24) allows to present resultant values of heat transfer coefficient against equilibrium values of quality x_e

2.3. Determination of shear stresses and heat transfer coefficient

The shear stresses distribution in the mist flow will now be analysed. According to the hypothesis put forward earlier by authors that is required in order to determine the heat transfer coefficient basing on the analogy between exchange of momentum and heat. Our earlier analysis in this paper enabled determination of the shear stresses at the interface between the two-phase core and the vapour phase. Due to evaporation of droplets from the core the two-phase mixture accelerates and the shear stresses increases with respect to the vapour flow only. Hence presence of two phase flow with liquid droplets in the core creates additional to the annular vapour flow shear stresses on the interface radius between the core and the vapour annulus and hence the additional source of energy dissipation.

The principle of momentum conservation in the single phase pipe flow returns the linear distribution of shear stress. The analysis presented above enables determination of the shear stress at the core-vapour interface, but the procedure to extrapolate it to the wall value is required. That is required for the sake of consistency of the hypothesis of summation of dissipation energy, which is applied to the flow in the boundary layer. It is assumed therefore that the difference between the core two phase shear stresses and existing shear stresses from vapour shear stress distribution at the core - vapour interface $\tau_{TP,M}(r_i)-\tau_v(r_i)$ is the additional contribution to energy dissipation in the boundary layer, which should be transferred to the wall as is shown in Fig. 2. Additional to the vapour only dissipation of energy is equal to the difference between dissipation energy of the two-phase flow at the core radius and the value corresponding to energy dissipation at the core radius due to vapour only flow. Total dissipation of energy should be evaluated in the boundary layer, hence the value of difference between the two-phase flow shear stress and vapour on the radius r is expressed by the value of the wall radius R.

Total shear stress on the wall yields:

$$\tau_{TP,M}(r_i) = \tau_v(r_i) + \Delta\tau_{TP,M}(r_i) = \tau_v(r_i) + \left(\frac{r_i}{R}\right)\left[\tau_{TP,M}(r_i) - \tau_v(r_i)\right] \tag{25}$$

Energy dissipation in the laminar sublayer close to the wall according to the hypothesis of energy dissipation (1) can be expressed as a ratio of the square of shear stress to the dynamic viscosity. Taking advantage of relation (3) we can derive from the relation describing the hypothesis of energy dissipation:

$$\tau_{TP,M,w}{}^2 = \tau_{w,v}{}^2 + \left[\tau_{TP,K}{}^2(r_i) - \tau_v^2(r_i)\right]\left(\frac{r_i}{R}\right)^2 \tag{26}$$

The two-phase flow shear stress can be calculated using definition of the single phase flow shear stress multiplied by the two-phase flow multiplier Φ^2:

$$\tau = f_{TPK}\tau_0 = \Phi^2 f \frac{\rho_0 w_0^2}{2} \tag{27}$$

We should underline that in all formulas for shear stresses velocities are the same and equal to the equivalent two-phase mist flow velocity because they correspond to the same homogenous flow (equivalent two-phase flow).

Substituting (27) into (26) we obtain the relation between the respective frictions coefficients taking into account (27):

$$f_{TP,M,w}{}^2 = f_{w,v}{}^2 + (f_{TPK}(r_i)^2 - f(r_i)_v^2)(\frac{r_i}{R})^2 \tag{28}$$

According to the Colburn analogy between heat and momentum transfer:

$$\frac{Nu}{\mathrm{Re}\,\mathrm{Pr}} = \frac{f}{2} \tag{29}$$

We can introduce (29) into (28) and find equivalent heat transfer coefficient for post dry out conditions (mist flow)

$$\alpha_{TPB,M}{}^2 = \alpha_{w,v}{}^2 + \left[\alpha_{TP,K}(r)^2 - \alpha_v(r)^2\right]\left(\frac{r}{R}\right)^2 \tag{30}$$

or

$$\frac{\alpha_{TPB,M}}{\alpha_{w,v}} = \sqrt{1 + \frac{\left[\alpha_{TP,K}(r)^2 - \alpha_v(r)^2\right]}{\alpha_{w,v}{}^2}\left(\frac{r}{R}\right)^2} \tag{31}$$

Relation (31) fulfils expected boundary conditions, i.e.:

$$for \quad r = 0 \quad \alpha_{TPB,M} = \alpha_{w,v} \tag{32a}$$

and

$$for \quad r = R \quad \alpha_{TPB,M} = \alpha_{TP,K}(R) \tag{32b}$$

Where, treating core flow as homogenous mixture:

$$\alpha_{TPB,K} = 0.023\,\mathrm{Re}_{TP,i}^{0.8}\,\mathrm{Pr}_{TP}^{0.4}\,\frac{\lambda_{TP}}{2R} \text{ where } \mathrm{Re}_{TP,i} = \frac{2w_{TP}(r_i)R}{\nu_{TP}} \tag{33}$$

And for vapour flow:

$$\alpha_v(r) = 0.023\,\mathrm{Re}_v^{0.8}\,\mathrm{Pr}_v^{0.4}\,\frac{\lambda_v}{2R} \text{ where } \mathrm{Re}_v = \frac{2w_{TP}(r_i)R}{\nu_v} \tag{34}$$

$$\alpha_{w,v} = 0.023\,\mathrm{Re}_{w,v}^{0.8}\,\mathrm{Pr}_v^{0.4}\,\frac{\lambda_v}{2R} \text{ where } \mathrm{Re}_{w,v} = \frac{2w_{TP}(R)R}{\nu_v} \tag{35}$$

Having the relation between the radius of interface and velocity against distance (17) and (22) or against quality (24) we can calculate heat transfer coefficient for post dryout in channel (31). Subsequently we can calculate temperature of the wall T_w:

$$T_w = \frac{q_w}{\alpha_{TPB,M}} + T_{sat} \tag{36}$$

3. Results of calculations and comparison with available experimental data.

The performance of the model presented above is evaluated in this section. First, detailed information of the velocity distribution in longitudinal direction of the channel is analysed. Calculations have been accomplished for three different values of the parameter a defined in equation (17), Fig. 4. A significant influence of that parameter is observed in modifications of the velocity profile. Next attention is focused on the distribution on the non-dimensional distance z^+ against non-dimensional radius r+. The results are presented in Fig. 5. In that figure exact expressions for the dependence $z^+=f(r^+)$, eq. (22), are plotted together with some approximation (denoted in the figures as fits, i.e. $z^+=-\ln(r^+)/A$). The two distributions are very consistent until $r^+\approx0.8$. Beyond that value the discrepancy increases markedly. Nevertheless, ignoring remaining terms on the right hand side of equation (20) results in the possibility of obtaining the analytical function describing the relation $r^+=r^+(z^+)$, indispensable for other calculations at the expense of an acceptable error. That assumption has been tested for potential examination of the case where the function $r^+=f(z^+)$ would be necessary. Otherwise implicit equation (22) should be solved numerically to obtain such function. In Fig. 6-8 presented are calculations distributions of non-dimensional heat transfer coefficient ratio versus non-dimensional radius at different mass velocities, obtained at constant wall heat flux, wall temperature and radius versus quality. In Fig. 6 is therefore shown the effect of varying mass velocity on heat transfer. In analyses the diameter of the tube and the heat flux were kept constant (d=0.015m, $q=10^6$ W/m$^{2)}$. The higher the value of heat flux the shorter is the distance of complete evaporation of the core flow. In calculations of thermal conductivity,

$\lambda_{TP,}$ the approach similar to that for the density ρ_{TP} is applied (equation (17)). Calculations have been executed at the constant value of the heat flux and tube diameter, for three different values of mass velocity G=500, 1500 and 2500 kg/(m^{2}s) and d=0.015m, respectively. As can be observed, the increase of mass flux leads to increased values of the heat transfer coefficient. In Fig. 7 presented are distributions of corresponding wall temperature. The corresponding distribution of radius with respect to quality is presented in Fig. 8.

In literature there exists a number of empirical post-dryout heat transfer correlations enabling determination of heat transfer coefficient. They are simple in use but have a limited range of validity and should not be extrapolated outside the recommended range. Some of most known of them have been selected for comparisons in the present study and are presented below.

The correlation due to Groeneveld [11] reads:

$$\alpha_{TPB,GR} = 0.00109\left\{\frac{Gd}{\mu_v}\left[x+\frac{\rho_v}{\rho_l}(1-x)\right]\right\}^{0.989}\mathrm{Pr}_w^{1.41}\frac{\lambda_v}{d}\left[1-0.1\left(\frac{\rho_l}{\rho_v}-1\right)^{0.4}(1-x)^{0.4}\right]^{-1.15} \quad (36)$$

The correlation due to Dougall and Rohsenow respectively [11].

$$\alpha_{TPB,DR} = 0.023\left\{\frac{Gd}{\mu_v}\left[x+\frac{\rho_g}{\rho_l}(1-x)\right]\right\}^{0.8}\mathrm{Pr}_v^{0.4}\frac{\lambda_g}{d} \quad (37)$$

Another correlation used in comparisons is the one due to Condie and Bengston [12]:

$$\alpha_{TPB,CB} = 0.05345\times10^{-3}\frac{\left(\lambda_g\times1000\right)^{0.4593}\mathrm{Pr}_w^{2.2598}\mathrm{Re}_v^{[0.6249+0.2043\ln(1+x)]}}{d^{0.8095}(x+1)^{2.0514}} \quad (38)$$

The correlation due to Wojtan et al [13] assumes the form:

$$\alpha_{TPB,Woj\,\tan} = 0.00117\left(\frac{Gd}{\mu_v}\right)^{0.79}\mathrm{Pr}_v^{1.06}\frac{\lambda_v}{d}\left[1-0.1\left(\frac{\rho_l}{\rho_v}-1\right)^{0.4}(1-x)^{0.4}\right]^{-1.83} \quad (39)$$

Finally the correlation due to Sindhuja et al [14] has been tested:

$$\alpha_{TPB,Sindhuja}=0.0071\left\{\left(\frac{Gd}{\mu_l(T_f)}\right)\left[x+\frac{\rho_v}{\rho_l}(1-x)\right]\right\}^{1.154}\mathrm{Pr}_v^{0.577}\frac{\lambda_v}{d}\left(\frac{\lambda_l(T_f)}{\lambda_v}\right)^{0.59}\left(\frac{G^2}{\rho_l^2 gD}\right)^{0.0396}\left(\frac{q_w}{HG}\right)^{0.44}\left(\frac{T_{sat}}{T_{cr}}\right)^{-2.17}\left(p_r^{0.212}(1-p_r)\right)^{-0.27} \quad (40)$$

Some more empirical correlations can be found in Mayinger and Schnittger [15].

Present model is devised for use under conditions where dryout is developing in the channel. The location of dryout can be predicted from a correlation due to Levitan and Lantsman (pressure in Pa) [11]:

$$x_{CHF}=\left[0.39+1.57\left(\frac{p_{sat}}{98}\right)-2.04\left(\frac{p_{sat}}{98}\right)^2+0.68\left(\frac{p_{sat}}{98}\right)^3\right]\left(\frac{Gd}{1000}\right)^{-0.5}\left(\frac{8\times10^{-3}}{d}\right)^{0.15} \quad (41)$$

It is also possible to determine the location of dryout from the models devised by Wojtan et al [16] or Sun and Groll [17]. The correlation due to Wojtan et al. [16] returns similar predictions as the correlation due to Levitan and Lantsman, whereas the model dye to Sun and Groll [17] significantly overtshoots the location of dryout.

Some comparisons of the results have been made with the above mentioned empirical correlations described by equations (36) – (40). Empirical correlations are generally limited to particular flow conditions. Models known from literature as well as empirical correlations poorly evaluate heat transfer for quality close to unity and in limit are not reaching vapour flow only. The results of heat transfer coefficient distributions have been presented in Fig. 9-11 for the case of water for three values of mass velocity, i.e. G=500, 1500 and 2500 kg/m^{2}s. In Fig. 12-13 presented are the results for R134a for G=500 and 1000 kg/m^{2}s, whereas in Fig. 14-15 presented are the results of heat transfer calculations for R245fa for mass velocity G=500 and 1000 kg/m^{2}s. In all cases the similar value of the reduced pressure has been

selected, namely p_r=0.32. The postulated in the paper method described by equation (30) shows consistent results with the considered empirical correlations. In case of water a very good consistency of the presented model with the correlation due to Dougall and Rohsenow and Wojtan et al is obtained. It is worth to notice that only our correlation has proper asymptotic trends, because it reaches vapour flow heat transfer coefficient value, when the two -phase core is evaporated completely. In case of comparisons with the simulations for R134a and R245fa best consistency is obtained in comparison with the correlation due to Groeneveld.

4. Conclusions

On the base of detailed considerations of heat transfer processes occurring following the development of dryout in a channel flow a simple mechanistic heat transfer model for post-dryout dispersed flow regime has been developed. The model is suitable for calculation of the convective mechanisms of heat transfer in mist flow boiling. Model is developed on the basis of energy dissipation principle. A similar approach has been applied earlier by authors in the case of modelling of saturated and subcooled flow boiling [7-10]. In the presented case the radiation effects are omitted and the influence of pressure drop during the boiling flow on saturated temperature is also neglected. The suite of models [7-10] concerning the flow boiling in a channel are now supplemented by the model enabling determination of post dryout heat transfer. The presented model, in our opinion, is a useful contribution to the flow boiling modelling approached as together with the model for a subcooled and saturated boiling it is now enabling a full description of the flow boiling process in channels based on the same fundamentals, i.e. consideration of energy dissipation in the flow.

The model based on the energy dissipation principle has a general character. It can be used for estimation of heat transfer coefficients for different fluids, even these which have yet to be investigated experimentally from the heat transfer point of view.

Presented comparative analysis confirms satisfactory agreement in the regime of mist flow of the developed model for the considered fluids. The model attains the heat transfer coefficient value corresponding to only vapour flow for the complete evaporation of the drops in the core flow, which is hardly observed in the case of models known from literature as well as empirical correlations.

Obtaining better qualitative consistency of obtained formula (31) with experimental data is possible by introduction of the experimental correction factor related to the second term of the model, which modifies energy dissipation rendered by the presence of two-phase core flow.

Acknowledgements

The results presented in the paper have been partially funded from the project 2017/25/B/ST8/00755 by the National Science Centre, Poland.

References

1. Y. Guo Y., K. Mishima, A non-equilibrium mechanistic heat transfer model for post-dryout dispersed flow regime, Experimental Thermal and Fluid Science 26 (2002) 861–869.

2. K. Nishikawa, S. Yoshida, H. Mori, H. Takamatsu, Post-dryout heat transfer to Freon in a vertical tube at high subcritical pressures, Int. J. Heat Mass Transfer, vol. 29(8), (1986) 1245-1251.

3. O.C. Jones Jr., N. Zuber, Post-CHF Heat Transfer: A Non-Equilibrium, Relaxation Model, ASME Paper 77-HT-79, 1979.

4. V. I. Terekhov, M.A. Pakhomov, A.V. Chichindaev, Heat transfer in a tube laminar steam-drop flow, Thermophysics and Aeromechanics, vol. 7(4), (2000) 499-511.

5. V. Caha, J. Krejcí, Post critical heat transfer and fuel cladding oxidation, Acta Polytechnica CTU Proceedings 4:8–12, 2016.

6. H. Li, H. Anglart, Prediction of dryout and post-dryout heat transfer using a two-phase CFD model, Int. J. of Heat and Mass 99, (2016) 839–850.

7. J. Mikielewicz, Semi-empirical method of determining the heat transfer coefficient for subcooled saturated boiling in a channel, Int. J. of Heat and Mass Transfer, 17, (1973) 1129–1134.

8. D. Mikielewicz, J. Mikielewicz, A common method for calculation of flow boiling and flow condensation heat transfer coefficients in minichannels with account of nonadiabatic effects, Heat Transfer Engineering, 32, (2011) 1173-1181.

9. D. Mikielewicz, R. Andrzejczyk, B. Jakubowska, J. Mikielewicz, Comparative study of heat transfer and pressure drop during flow boiling and flow condensation in minichannels, Heat Transfer Engineering, vol. 37(13-14), (2016) 1158-1171.

10. J. Mikielewicz, D. Mikielewicz, A simplified energy dissipation based model of heat transfer for subcooled flow boiling, Int. J. of Heat and Mass Transfer, 106, (2017) 280–288.

11. V. P. Carey, Liquid-Vapour Phase-Change Phenomena, An Introduction to the Thermophysics of Vaporisation and Condensation Processes in Heat Transfer Equipment, Hemisphere, 1992.

12. S-K. Moon, S-Y. Chun, S. Cho, S-Y. Kim, W-P. Baek, An experimental study on post-CHF heat transfer for low flow of water in a 3×3 rod bundle, Nuclear Engineering and Technology, vol. 37(5), 457-468, 2005.

13. Sindhuja, R., Balakrishnan, A., Murthy, S. S., Post-CHF heat transfer during two-phase upflow boiling of R-407C in a vertical pipe. Applied Thermal Engineering 30, 167 – 173, 2010.

14. Wojtan, L., Ursenbacher, T., Thome, J.R., Investigation of flow boiling in horizontal tubes: Part II - development of a new heat transfer model for stratified-wavy, dryout and mist flow regimes. International Journal of Heat and Mass Transfer 48 (14), 2970 – 2985, 2005.

15. F. Mayinger, R. Schnittger, Post-Dryout Heat Transfer in Tubes with Uniform and Circumferentially Nonuniform Heating, Current researches in heat and mass transfer, eds.: K. Murthy et al. Washington: Hemisphere Publ. Corp., Berlin: Springer-Verlag, 157-165, 1986.

16. Wojtan, L., Ursenbacher, T., Thome, J.R., Investigation of flow boiling in horizontal tubes: Part I - a new diabatic two-phase flow pattern map. International Journal of Heat and Mass Transfer 48 (14), 2955 –2969, 2005.

17. Sun, Z., Groll, E., CO2 flow boiling heat transfer in horizontal tubes. Part 1: flow regime and prediction of dry-out. Proceedings of 5th IIR-Gustav Lorentzen Conference on Natural Working Fluids. 131 –140, 2002.

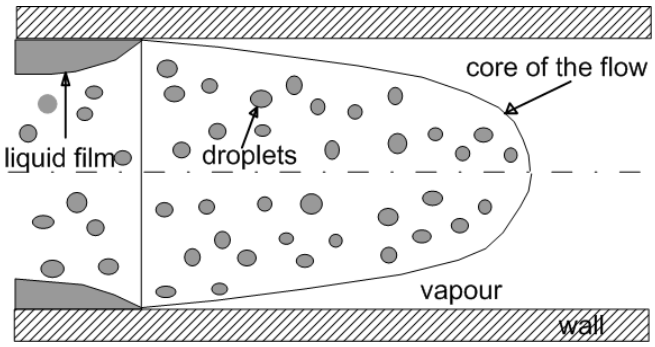

Fig. 1. Schematic of the diminishing liquid film in an annular flow and beginning of post-dryout heat transfer.

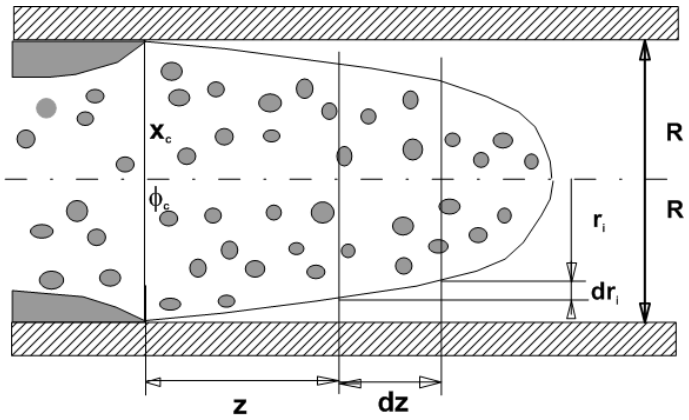

Fig. 2. Post dryout schematic of heat transfer

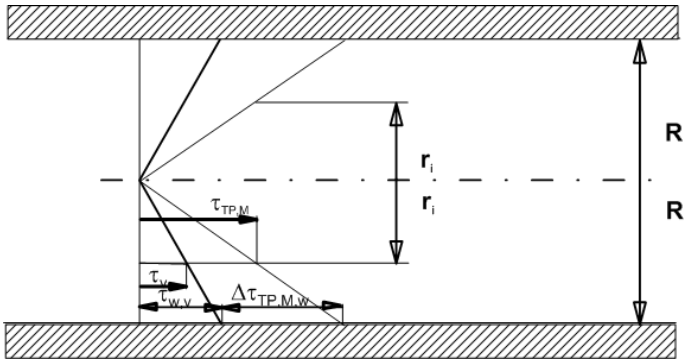

Fig. 3. Schematic of distribution of shear stress in equivalent two-phase mist flow in the core and annular vapour flow in the remaining part of the cross-section.

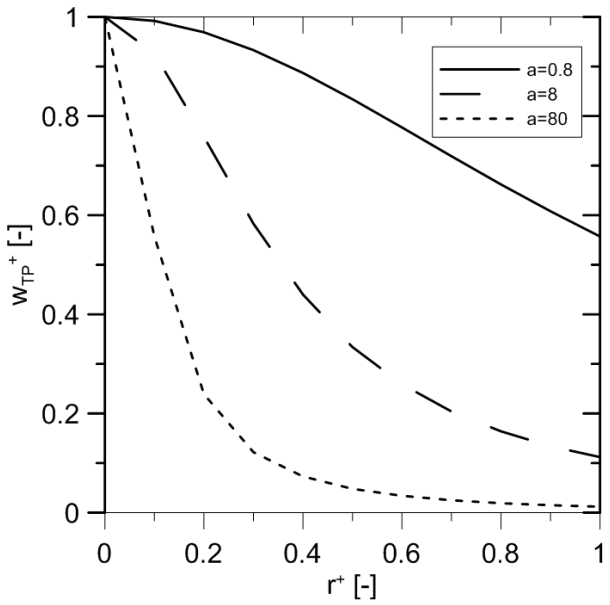

Fig. 4 Distributions of non-dimensional two-phase flow velocity in function of non-dimensional radius for different values of the parameter a, equation (17).

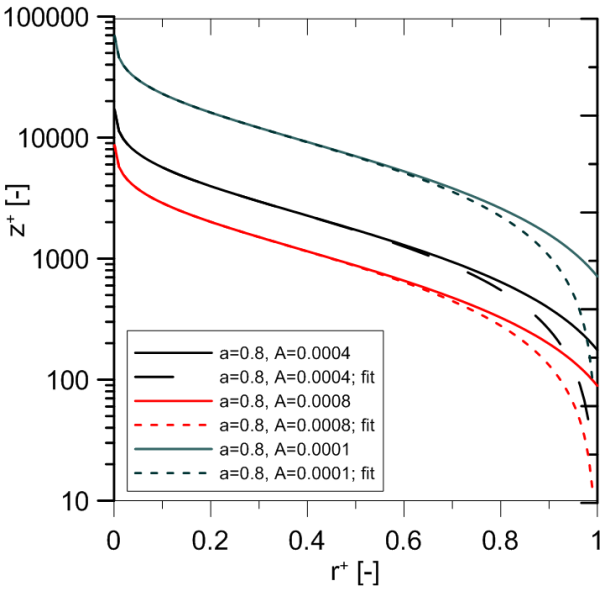

Fig. 5. Distributions of non-dimensional distance versus non-dimensional radius in comparisons to approximation functions, equation (22).

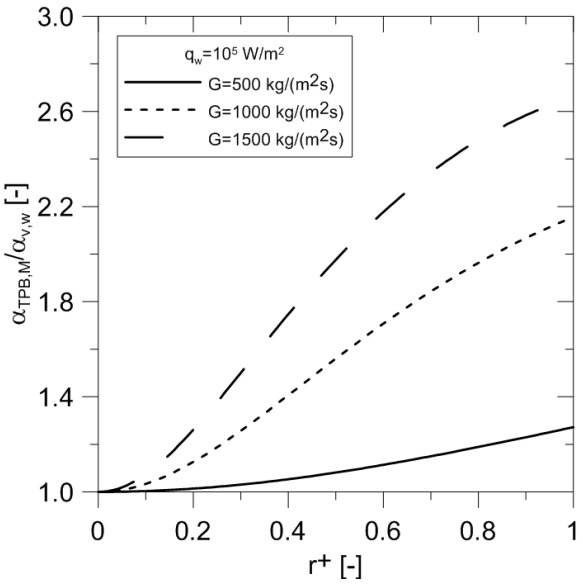

Fig. 6. Distributions of non-dimensional heat transfer coefficient ratio versus non-dimensional radius at different mass velocities (constant wall heat flux), equation

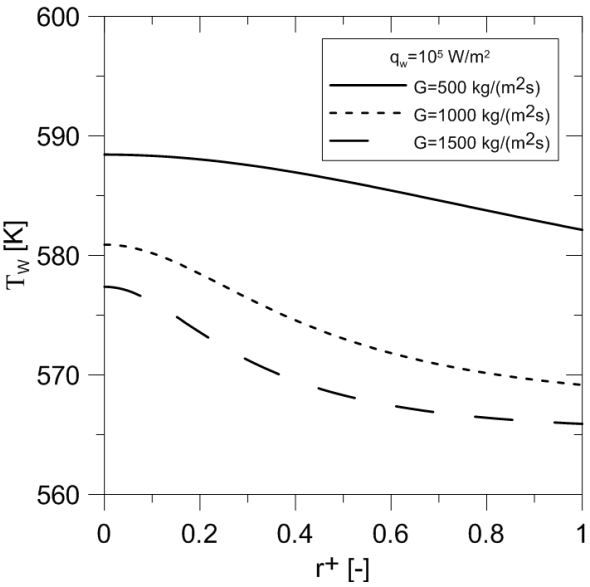

Fig. 7 Distributions of wall temperature versus non-dimensional radius at different mass velocities (constant wall heat flux), equation (29).

(31).

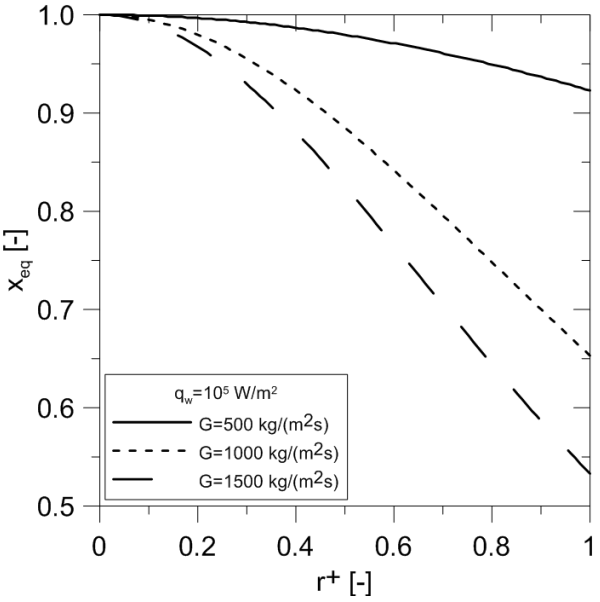

Fig. 8 Radius of core flow against equilibrium quality equation (24)

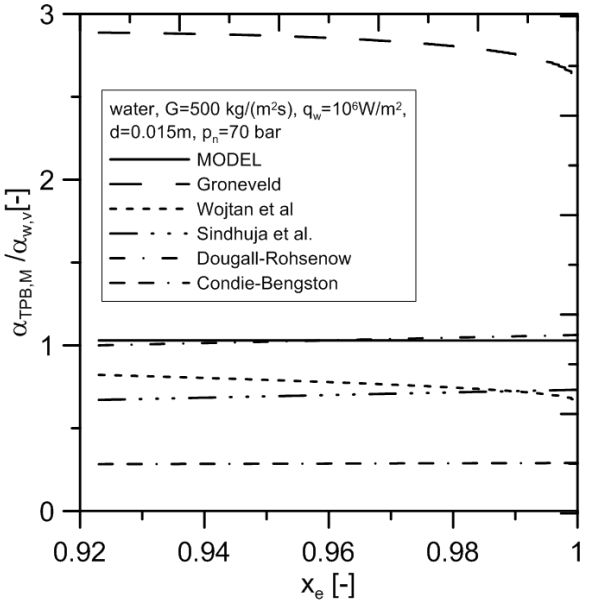

Fig.9. Comparison of the model with a number of empirical correlations in the case of water.

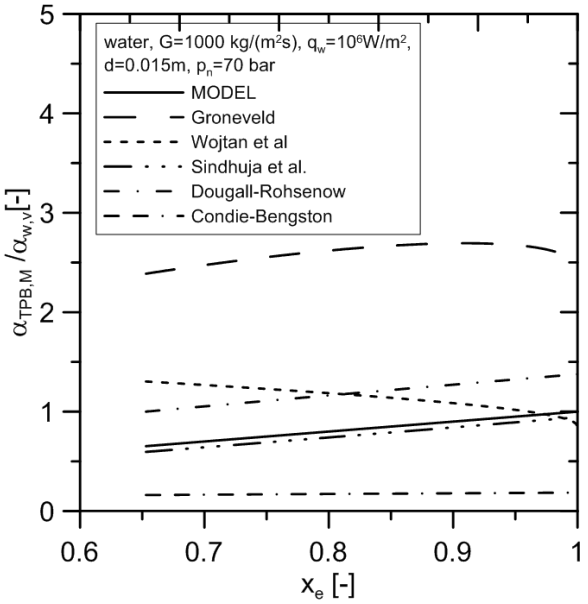

Fig. 10. Distributions of heat transfer coefficient ratio versus quality at constant mass velocity (constant wall heat flux), equation (30).

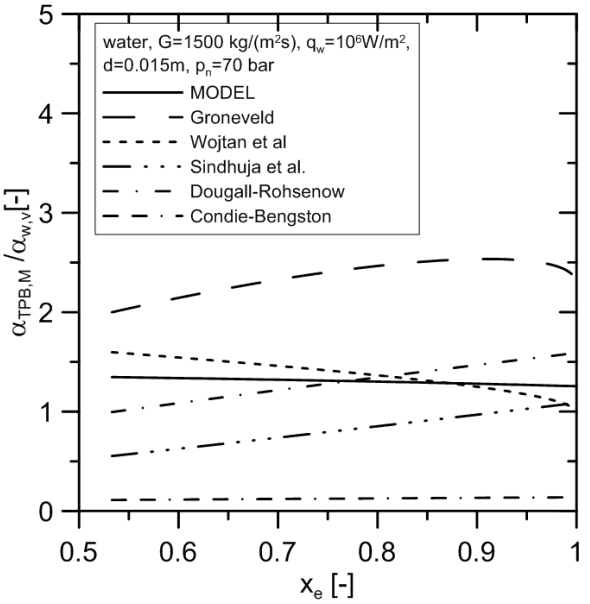

Fig. 11. Distributions of heat transfer coefficient ratio versus quality at constant mass velocity (constant wall heat flux), equation (29).

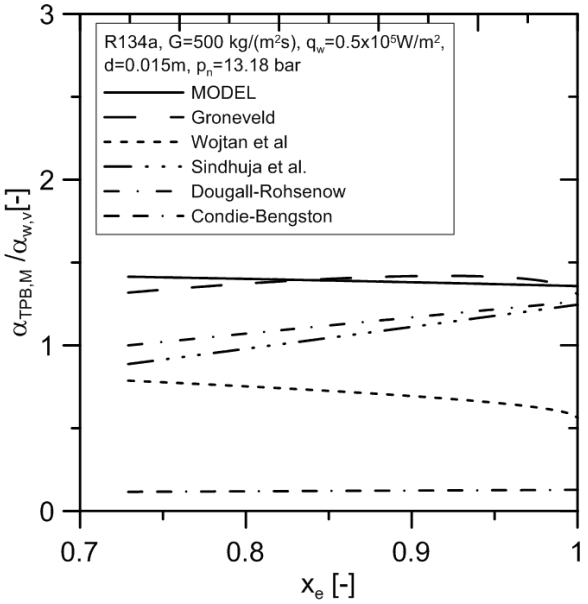

Fig. 12. Distributions of heat transfer coefficient ratio versus quality at constant mass velocity (constant wall heat flux), equation (29).

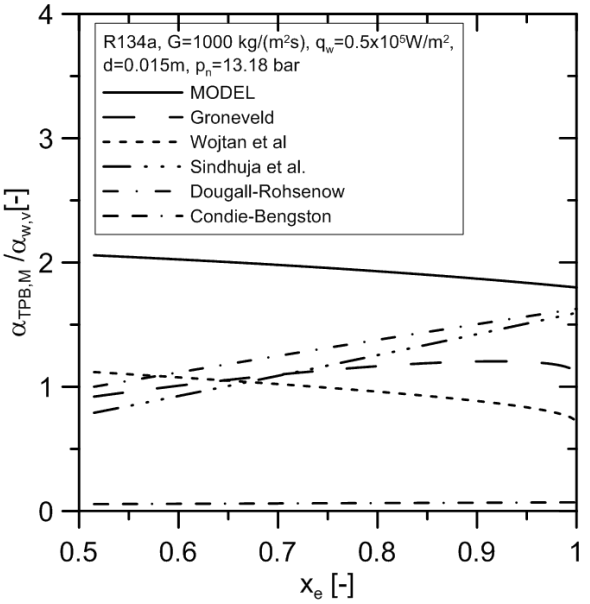

Fig. 13. Distributions of heat transfer coefficient ratio versus quality at constant mass velocity (constant wall heat flux), equation (29).

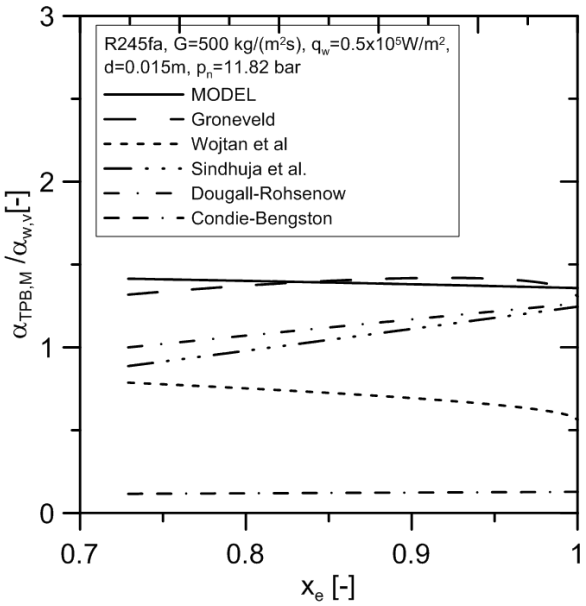

Fig. 14. Distributions of heat transfer coefficient ratio versus quality at constant mass velocity (constant wall heat flux), equation (29).

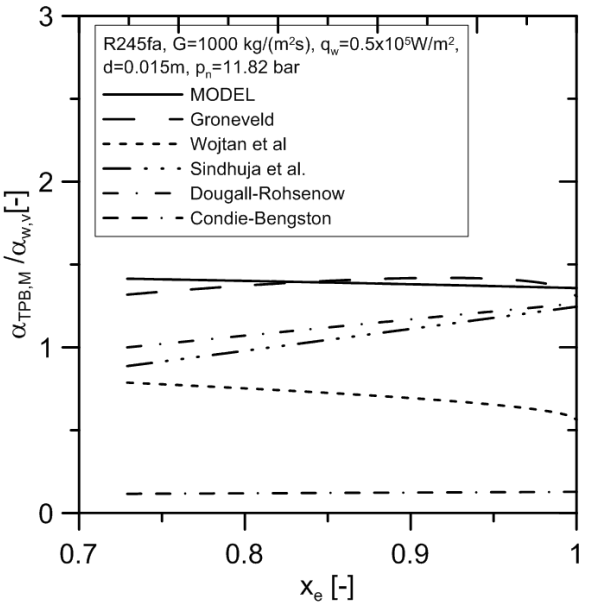

Fig. 15. Distributions of heat transfer coefficient ratio versus quality at constant mass velocity (constant wall heat flux), equation (29).